

A junction coverage compatibility score to quantify the reliability of transcript abundance estimates and annotation catalogs

Charlotte Sonesson^{1,2,*}, Michael I Love^{3,4}, Rob Patro⁵, Shobbir Hussain⁶,
Dheeraj Malhotra⁷ and Mark D. Robinson^{1,2,*}

¹ Institute of Molecular Life Sciences, University of Zurich, 8057 Zurich, Switzerland

² SIB Swiss Institute of Bioinformatics, University of Zurich, 8057 Zurich, Switzerland

³ Department of Biostatistics, UNC-Chapel Hill, Chapel Hill, NC, US

⁴ Department of Genetics, UNC-Chapel Hill, Chapel Hill, NC, US

⁵ Department of Computer Science, Stony Brook University, NY, US

⁶ Department of Biology and Biochemistry, University of Bath, Bath BA2 7AY, United Kingdom

⁷ F. Hoffmann-La Roche Ltd , Pharma Research and Early Development (pRED), Neuroscience, Ophthalmology and Rare Diseases (NORD), Roche Innovation Center Basel, 4070 Basel, Switzerland

* Correspondence to charlotte.sonesson@uzh.ch or mark.robinson@imls.uzh.ch

Abstract

Most methods for statistical analysis of RNA-seq data take a matrix of abundance estimates for some type of genomic features as their input, and consequently the quality of any obtained results are directly dependent on the quality of these abundances. Here, we present the junction coverage compatibility (JCC) score, which provides a way to evaluate the reliability of transcript-level abundance estimates as well as the accuracy of transcript annotation catalogs. It works by comparing the observed number of reads spanning each annotated splice junction in a genomic region to the predicted number of junction-spanning reads, inferred from the estimated transcript abundances and the genomic coordinates of the corresponding annotated transcripts. We show that while most genes show good agreement between the observed and predicted junction coverages, there is a small set of genes that do not. Genes with poor agreement are found regardless of the method used to estimate transcript abundances, and the corresponding transcript abundances should be treated with care in any downstream analyses.

Keywords: RNA-seq, Abundance quantification, Reliability, Quality control

27 Introduction

28 High-throughput sequencing of the transcriptome (RNA-seq) is used for a broad range of applications in biol-
29 ogy and medicine. Most of these involve comparing expression levels of genetic features (e.g., genes, transcripts
30 or exons) between samples, and the quality of the results from any such study will therefore be directly depen-
31 dent on the correctness of the expression estimates for the particular features of interest. The ability to obtain
32 accurate estimates, in turn, depends on the quality and quantity of the available data, as well as the complete-
33 ness and correctness of the utilized reference annotation. In general, reliable abundance estimation is easier to
34 achieve for genes than for individual transcripts or isoforms, due to the high sequence similarity among groups
35 of isoforms and the non-uniform read coverage resulting from library preparation and sequencing biases [1, 2].
36 However, gene-level abundance estimation is not without challenges, particularly for groups of genes that share
37 a large fraction of their sequence, which leads to high numbers of multimapping reads [3–5]. Various solutions
38 have been proposed, including grouping together similar genes [4], probabilistic assignment of reads to genes
39 [3] and scoring the genes based on their sequence similarity and number of multi-mapping reads shared with
40 other genes [5].

41 Despite their higher reliability, gene-level abundances are insufficient for analyses aimed at detecting dif-
42 ferences in transcript-level expression or relative isoform usage. Even for studies where the main aim is to
43 detect differential expression on the gene level, incorporating transcript abundances can in some cases improve
44 the inference [2, 6, 7]. As methods for transcript abundance estimation are improving, both in accuracy and
45 speed, it has become increasingly common to estimate abundances of individual isoforms rather than of the
46 gene as a whole, and today a plethora of transcript abundance estimation methods based on various under-
47 lying algorithms are available (e.g., [8–17]). Most evaluations of the ability of these methods to accurately
48 estimate transcript abundances have been performed using simulated data, where reads are generated from a
49 known transcriptome [1, 2], or using artificial spike-in sequences [18]. Evaluations have also been done based
50 on the agreement of abundance estimates between replicates [19] or agreement with abundances or abun-
51 dance ratios derived from other types of data such as exon arrays [20], RT-PCR [21] or 3' end sequencing [1].
52 Less is known about the reliability of transcript abundance estimates in real data sets, based on potentially
53 inaccurate or incomplete annotation catalogs, and how to spot unreliably quantified transcripts in a sample-
54 wise manner based on the RNA-seq data alone. A motivating example is illustrated in Figure 1A, showing
55 abundance estimates for the ZADH2 gene in EBV-transformed lymphocytes, as displayed in the GTEx Portal
56 (<https://www.gtexportal.org/home/gene/ZADH2>, accessed July 19, 2018). This gene has four annotated iso-
57 forms, each consisting of two exons and each featuring a unique splice junction (with a shared acceptor site).
58 The top row illustrates the estimated expression of collapsed exons and junctions (with legends to the right),
59 indicating a high expression of the most 5' exon and the corresponding junction. The alternative exons and
60 junctions have no or very few supporting reads. However, the isoform abundance estimates (lower panel) sug-
61 gest a different picture, where two of the isoforms whose unique exons and junctions are supported by few
62 reads are assigned the highest expression levels.

63 In this paper, we present the junction coverage compatibility (JCC) score (Figure 1B), which allows auto-
64 mated detection of genes with conflicting indications of isoform abundance. The score can be calculated for
65 any genomic region (e.g., a gene locus), by comparing the observed coverage profile, obtained by aligning the
66 RNA-seq reads to the genome, with the predicted coverage profile derived from estimates of transcript abun-
67 dances and biases influencing the observed read coverage of a sequenced transcript. In particular, we focus on
68 the number of reads spanning annotated splice junctions in the genomic region of interest. The key assumption
69 behind the JCC score is that with (i) a complete and accurate catalog of reference transcripts, (ii) an accurate
70 estimate of the abundance of each individual transcript, and (iii) knowledge about the biases affecting the prob-

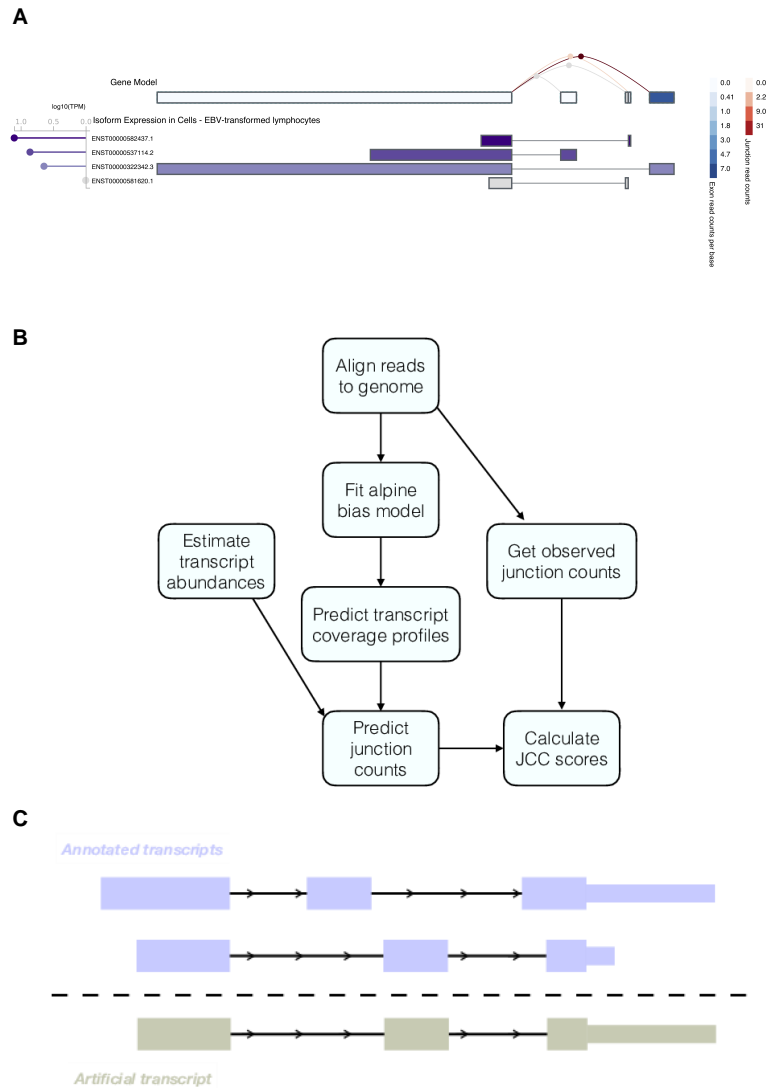


Figure 1: **A.** Example of a gene with inconsistent signals resulting from abundance estimation based on exons, junctions or entire isoforms. The figure was generated in the GTEx Portal (<https://www.gtexportal.org/home/gene/ZADH2>, accessed July 19, 2018). **B.** Outline of the approach used to calculate the JCC scores. First, reads are aligned to the genome using STAR, and the number of reads observed to span each annotated splice junction is extracted. The aligned reads are also used to fit a fragment bias model using the *alpine* Bioconductor package, which is then used to predict coverage profiles for all annotated transcripts. The coverage profiles are combined with transcript abundance estimates to obtain the predicted numbers of junction-spanning reads, which are compared to the observed numbers to calculate the JCC score for each gene. **C.** Schematic illustrating the generation of artificial transcripts in the simulated data. In total, artificial transcripts are generated for 4,514 genes, which have multiple annotated 3'UTR of different length (at least 1kb length difference) starting in the same genomic position. For each such gene, two transcripts are selected; one that is annotated with the short 3'UTR and one that is annotated with the long one. The artificial transcript is created by combining the internal structure (all exonic regions except the annotated 3'UTR) of one of the two isoforms with the 3'UTR of the other. In the simulation, all reads from the modified genes are generated from the artificial transcripts.

71 ability of a given fragment of a given transcript to be sequenced, the coverage profile prediction obtained by
72 combining these three sources of information for any genomic locus should be close to the observed one. Thus,
73 large deviations between the observed and predicted coverage profiles indicate that the transcript estimates
74 in the region are unreliable, and such regions should be flagged and interpreted with caution in downstream
75 analysis. There can be many reasons behind a region obtaining a high (bad) JCC score, ranging from poor
76 performance of the estimation method, e.g. due to sequence similarity with other parts of the transcriptome, to
77 an incorrect or incomplete annotation catalog, making a correct distribution of the reads between the annotated
78 transcripts in the region impossible.

79 Using eight transcript abundance estimation methods and two deeply sequenced human RNA-seq data
80 sets, we show that for the majority of the human genes, the junction coverages predicted from the transcript
81 abundances are highly compatible with the observed junction coverages, suggesting overall accurate annotation
82 and transcript abundance estimates. However, a small fraction of the annotated genes show a substantial
83 difference between the predicted and observed junction coverages. For some of these genes, the reason for the
84 incompatibility appears to be an incompletely annotated transcript catalog, and no distribution of the reads
85 among the annotated isoforms would simultaneously give a satisfactory junction coverage compatibility and
86 a good agreement with the annotated UTRs. The uneven read coverage of isoforms also leads to estimation
87 problems, especially for genes with short, poorly covered exons. Using a simulated data set, we show that
88 misannotation of 3'UTRs can lead to unreliable transcript estimates, which is interesting in the light of recent
89 reports showing that the majority of isoform differences between tissues are due to alternative start and end
90 sites and involve untranslated exons [22–24].

91 **Materials and Methods**

92 **Experimental data and reference annotations**

93 We use two deeply sequenced human polyA+ RNA-seq libraries for our investigations. The first (*Cortex*)
94 contains 117,292,547 paired-end 126nt Illumina reads from a human cerebral cortex sample, and the second
95 (*HAP1*) contains 55,234,720 paired-end 151nt Illumina reads from the HAP1 cell line. Both samples were
96 prepared with the Illumina TruSeq RNA stranded protocol and sequenced at the Functional Genomics Center
97 in Zurich, Switzerland; *Cortex* with a HiSeq 2500 in October 2015 and *HAP1* with a HiSeq 4000 in September
98 2017. Raw FASTQ files have been uploaded to ArrayExpress (accession number E-MTAB-7089). Most of our
99 analyses are performed using the GRCh38.90 reference annotation from Ensembl [25]. For comparison, we
100 also use the recent CHES 2.0 reference catalog [26], which was generated by assembling RNA-seq reads from
101 almost 10,000 GTEx samples [27, 28] using StringTie [14]. Based on the original Ensembl gtf file, we generate
102 two additional gtf files, containing flattened exonic regions and intronic regions (regions within a gene locus
103 that are not covered by any exon), respectively, and use featureCounts [29] (from subread [30] v1.6.0) to count
104 the number of reads overlapping these exonic and intronic regions for each gene.

105 **Simulated data**

106 In addition to the experimental RNA-seq data sets, we generate synthetic data with the aim to better understand
107 the effect of misannotated 3'UTR sequences. From the GRCh38.90 Ensembl annotation, we find 4,514 genes with
108 multiple annotated 3'UTRs starting in the same position, and with length difference exceeding 1kb. For each of
109 these genes, we randomly extract one transcript annotated with the short 3'UTR and one transcript annotated
110 with the long one. We then generate an artificial transcript, consisting of the 5'UTR and coding sequence of

111 one of these two transcripts and the 3'UTR of the other transcript (Figure 1C). For 41 of the 4,514 genes (0.9%),
112 the artificial transcript was identical to an annotated transcript (38 were identical to the transcript providing
113 the 3'UTR, 3 to other isoforms of the gene). These genes were not considered modified. We use the polyester
114 Bioconductor package [31] (v1.16.0) to simulate approximately 1,000 strand-specific read pairs (read length
115 125nt) from each of the 4,473 remaining artificial transcripts, and a total of 10 million read pairs distributed
116 between 10,000 randomly selected transcripts, not annotated to any of the genes from which the artificial
117 transcripts were generated. The simulated data set is then processed using the original Ensembl GRCh38.90
118 annotation files (which do not contain the artificial transcripts).

119 **Transcript abundance estimation**

120 We use eight methods to estimate abundances of the annotated transcripts in each of the two Illumina libraries:

- 121 • RSEM. We build an index from the combined cDNA and ncRNA reference fasta files from Ensembl,
122 and estimate transcript abundances with RSEM [9] (v1.3.0), using bowtie [32] (v1.1.2) as the underlying
123 aligner.
- 124 • Salmon. We build a transcriptome index from the combined cDNA and ncRNA reference fasta files
125 from Ensembl and run Salmon [16] (v0.11.0) in quasi-mapping mode, incorporating sequence, GC and
126 positional bias correction. We also generate 100 bootstrap samples for estimation of the inferential variance
127 for each transcript. By default, Salmon removes duplicated sequences in the reference catalog, keeping
128 only one representative. In this process, 12,824 transcripts from 4,499 genes were excluded from the
129 Ensembl GRCh38.90 catalog. In a majority of these cases, at least one of the identical sequences can be
130 found on an alternative contig (e.g., in the MHC region). It's worth noting that these contigs are not
131 included in the primary genome assembly used for the genomic alignments, while the transcripts are
132 contained in the Ensembl transcriptome fasta files. 3,450 of the affected genes did not have any other
133 annotated transcript and were thus completely removed from the annotation catalog.
- 134 • SalmonKeepDup. Here we run Salmon with the same settings as above, but retain all duplicated transcript
135 sequences in the catalog (which is an option during Salmon's indexing step). Since the retained transcripts
136 are sequence-identical, the estimated abundances will be uniformly distributed within groups of identical
137 transcripts.
- 138 • kallisto. We build a transcriptome index from the combined cDNA and ncRNA reference fasta files from
139 Ensembl, and run kallisto [15] (v0.44.0) with bias correction activated.
- 140 • Hera. The Hera index is built using the reference genome (primary assembly) and the Ensembl gtf file,
141 and Hera (<https://github.com/bioturing/hera>) (v1.1) is run with default settings.
- 142 • HISAT2+StringTie. We build a HISAT2 [33] (v2.1.0) index from the reference genome (primary assembly)
143 and extract the known splice sites using the provided `hisat2_extract_splice_sites.py` script. The
144 reads are aligned to this index with the option `--dta set` and given the known splice sites. Next, we run
145 StringTie [14] (v1.3.3b) without assembly of new transcripts (`-e` option) to get the abundance estimates
146 for the annotated transcripts.
- 147 • SalmonSTAR. For this approach we build a transcriptome index from the combined cDNA and ncRNA
148 reference files from Ensembl, and align the reads using STAR [34] (v2.5.3a). We subsequently estimate
149 transcript abundances using Salmon (v0.11.0) in alignment-based mode, incorporating sequence and GC
150 bias correction.

- 151 • SalmonCDS. Here, we build the Salmon index using only the explicitly annotated coding sequences from
152 Ensembl, and run Salmon (v0.11.0) in quasi-mapping mode, incorporating sequence, GC and positional
153 bias correction.

154 Prediction of expected junction coverage

155 In order to predict the expected number of reads mapping across each junction, given estimates of the transcript
156 abundances, we first fit a fragment-level bias model using the `alpine` Bioconductor package [35] (v1.2.0). The
157 bias model is fit for each library separately, using a set of single-isoform genes with length between 600 and
158 7,000 bp and between 500 and 10,000 assigned reads. The `alpine` bias model included random hexamer bias,
159 fragment GC bias, positional bias along the transcript, and the fragment length distribution. After fitting the
160 bias model, we use it to obtain a predicted coverage of each base pair in each annotated transcript using the
161 fitted parameters for these four factors. For transcripts where the prediction fails (e.g., transcripts shorter than
162 the estimated fragment length and transcripts with no overlapping reads), we assume a uniform coverage
163 rather than excluding them from subsequent analysis steps. Next, we rescale the predicted base pair coverages
164 by dividing with their total sum and multiplying with the average fragment length and the estimated transcript
165 counts from each of the transcript abundance estimation methods, in order to get an estimate of the number
166 of reads predicted to cover each position on the transcript. We also extract the position of annotated splice
167 junctions within each transcript, and the predicted coverage at the base just before an annotated junction is
168 used as the predicted number of reads from that transcript that align across the junction. Finally, we sum the
169 predicted number of junction-spanning reads for each junction across all transcripts, in a strand-aware fashion
170 (since the libraries are stranded) in order to get the total number of reads predicted to span any given junction.

171 Observed junction coverage

172 The observed junction coverage (the number of reads mapping across a given junction) is obtained using STAR
173 [34] (v2.5.3a). We build an index using the reference genome (primary assembly) and the Ensembl gtf file, and
174 align the reads with default settings. The number of uniquely mapping and multimapping reads spanning
175 each annotated junction are extracted from the SJ.out.tab output file from the STAR alignment.

176 The junction coverage compatibility score

177 To quantify the level of agreement between the predicted junction coverages based on any of the transcript
178 abundance estimation methods and the observed number of junction reads from STAR, we define a family of
179 gene-wise junction coverage compatibility (JCC) scores, parametrized by two arguments: a weighting function
180 g and a scaling indicator β (see below). For a given g and β , the JCC score for gene i is defined by

$$JCC_i = \frac{\sum_{j \in J_i} g(\omega_j) \left| \left(\frac{\sum_{k \in J_i} g(\omega_k) R_k}{\sum_{k \in J_i} g(\omega_k) C_k} \right)^\beta C_j - R_j \right|}{\sum_{j \in J_i} g(\omega_j) R_j}$$

181 where J_i denotes the set of junctions annotated to gene i (some junctions are annotated to transcripts from
182 multiple genes, in which case they are included for all of them), R_j is the observed number of uniquely mapping
183 reads spanning junction j (obtained from STAR) and C_j is the predicted number of reads spanning junction j
184 based on the bias model from `alpine` and the transcript abundances from a given method. Multimapping reads
185 (from STAR) cause problems in the score calculation since it is not clear how to assign them to junctions, and

186 thus the contribution of a junction is weighted by $g(\omega_j)$, where $g : [0, 1] \mapsto [0, \infty)$ is a non-negative function
187 and ω_j is the fraction of reads spanning junction j that are uniquely mapping.

188 Overall differences in the number of reads assigned to gene i by transcript abundance estimation compared
189 to junction counts can induce large differences between C_j and R_j even if their relative coverage patterns are
190 similar. The same is true if there is a large fraction of multimapping reads, which are being accounted for in
191 the predicted transcript abundances but not in the observed junction coverages. To account for this, we include
192 an optional scaling of the predicted coverages to have the same (weighted) sum as the observed coverages. This
193 is represented by the β parameter - if this is 0, no scaling is done, and if it is 1, the values are scaled. In this
194 study, we set $\beta = 1$, and let

$$g(\omega) = \begin{cases} 1 & \text{if } \omega \geq 0.75 \\ 0 & \text{otherwise} \end{cases}$$

195 i.e., a step function that implies that we only allow junctions with more than 75% uniquely aligning reads to
196 contribute to the JCC score calculations.

197 With $\beta = 1$, the JCC score for a gene takes values between 0 and 2. A low score means that the predicted
198 junction coverages, given the abundance estimates for the transcripts in gene i , are compatible with the observed
199 number of reads mapping across the junctions, while a high score indicates that for at least one junction, the
200 predicted number of junction-spanning reads does not match with the observed number.

201 Code availability

202 All code used to perform the analyses is available from [https://github.com/csoneson/annotation_problem_](https://github.com/csoneson/annotation_problem_txabundance)
203 `txabundance`.

204 Results

205 Predicted transcript coverage patterns agree well between samples

206 The prediction of the transcript coverage profiles by `alpine` is a crucial step in the calculation of the JCC
207 score. It is done separately for each of the two Illumina libraries, in order to account for any sample-specific
208 biases. Of the 200,310 annotated transcripts in the Ensembl gtf file, the prediction of the coverage pattern
209 by `alpine` returned an expected error for 29,342 (14.6%) in the *HAP1* sample and 13,906 (6.9%) in the *Cortex*
210 sample, almost exclusively due to transcripts being shorter than the respective fragment lengths. The prediction
211 returned NULL for 23,028 (11.5%) transcripts in the *HAP1* sample and 11,941 (6.0%) in the *Cortex* sample that
212 did not have any overlapping reads. For these transcripts we impose a uniform coverage, rather than excluding
213 them from subsequent calculations.

214 Overall, we observe a high correlation between the predicted coverage profiles in the two libraries (Supple-
215 mentary Figure 1), indicating that they share many of the biases, despite coming from different cell types and
216 being prepared and sequenced almost two years apart on different sequencing machines. The coverage predic-
217 tion is the single most time-consuming step of the JCC score calculation, and the high correlation even between
218 such different libraries suggests that in a specific study, the prediction may not need to be done separately for
219 each individual sample, which can reduce the run time considerably. Run time can also be reduced by limiting
220 the coverage prediction and subsequent analysis to transcripts from a subset of the genes that are of particular
221 interest in a given situation.

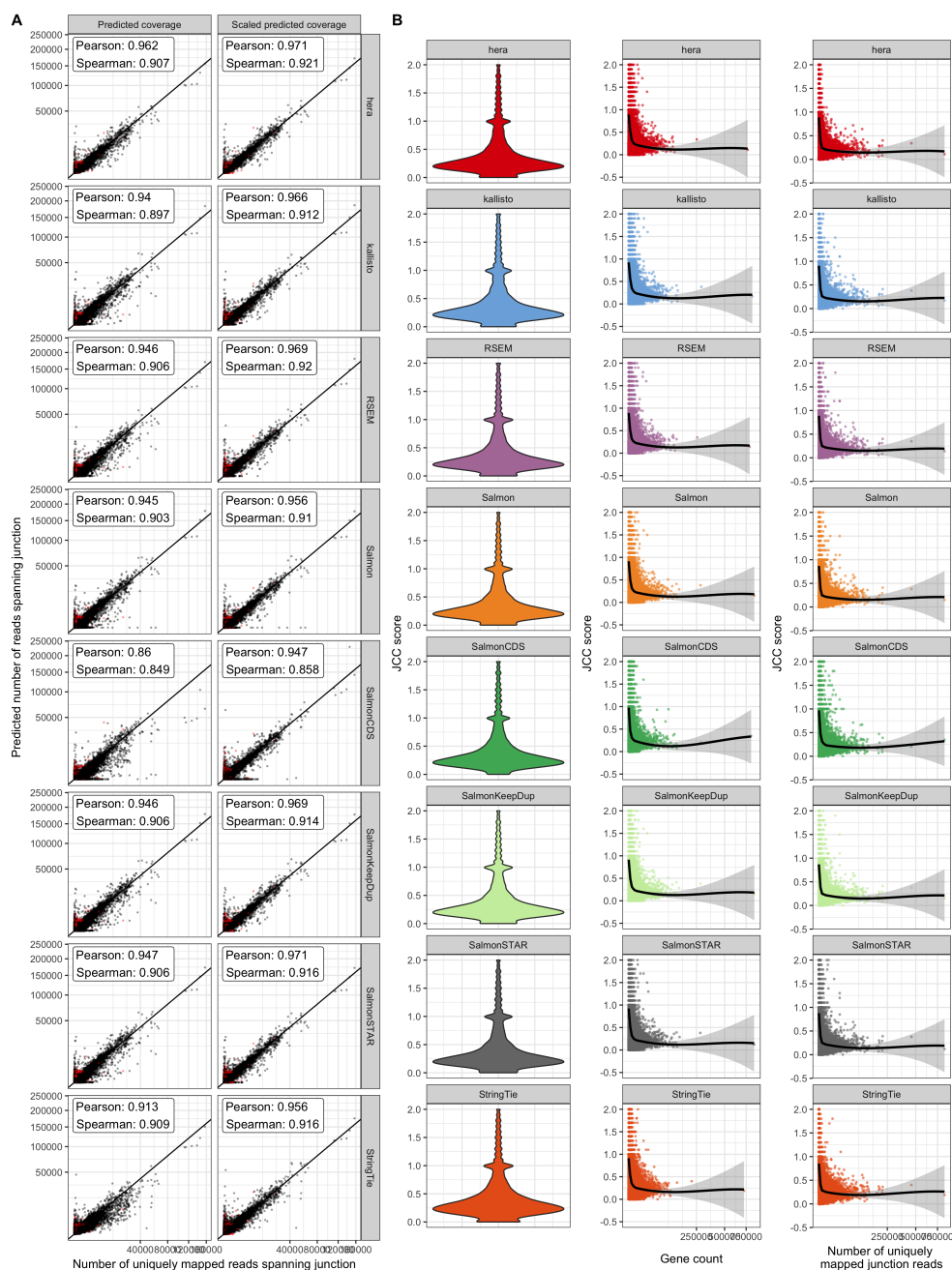


Figure 2: **A**. Correlation between observed and predicted number of reads spanning each junction for the *HAP1* sample. The left column (“Predicted coverage”) shows the actual number of reads predicted by *alpine*, while the predicted values in the right column (“Scaled predicted coverage”) are scaled to sum to the same number as the observed number of uniquely mapping junction reads within each gene. Scaling improves the correlation between observed and predicted junction coverages for all included methods. Axes are square-root transformed for better visualization. Red points indicate junctions where less than 75% of the spanning reads are uniquely mapping. **B**. Overall distribution of the gene-wise JCC scores for each method in the *HAP1* sample, as well as the association between the JCC score and the total number of reads for the gene and the number of uniquely mapped junction reads in the gene.

222 **Most predicted junction coverages are consistent with the observed coverages**

223 Using the approach described in the Methods section, we obtain the number of uniquely mapping reads ob-
224 served to span each annotated junction as well as the number predicted to span each junction given each set of
225 transcript abundance estimates. Comparing the predicted junction coverages C_j to the observed ones R_j across
226 all annotated junctions shows a generally high correlation for all abundance estimation methods (Figure 2A,
227 left column), suggesting that in most genomic loci, the annotated transcript structure is compatible with the
228 observed read alignments, and that the approach we use to predict junction coverages based on transcript
229 abundances is valid. Scaling the predicted junction coverages within each gene, corresponding to setting $\beta = 1$
230 in the subsequent JCC calculation and thereby focusing more on the relative junction coverages within a gene
231 rather than the overall abundance of the gene, increases the correlation for all methods (Figure 2A, right col-
232 umn). The largest discrepancies between observed and predicted junction coverages are seen for SalmonCDS,
233 indicating that on a global scale, only considering annotated coding sequences discards relevant information
234 about transcript abundances. We also note that there is a set of junctions with a low fraction of uniquely map-
235 ping reads (Figure 2A, marked in red) for which the predicted number of spanning reads is considerably higher
236 than the observed number of uniquely mapping junction reads. Since these discrepancies do not represent a
237 failure of the annotation system or transcript abundance estimation method, but rather an inability to place
238 reads in a unique genomic position, we downweight the influence of these junctions on the JCC score via the
239 $g(\omega)$ function, as described in the Methods section.

240 **Most genes show high compatibility between observed and predicted junction coverages**

241 After investigating the concordance between observed and predicted coverages for individual junctions, we next
242 calculate the JCC score for each annotated gene. With the exception of SalmonCDS (which is using a reference
243 annotation in which many transcripts and genes are missing since they don't have an explicitly annotated
244 coding sequence), we are able to calculate a valid JCC score for around 16,500 genes in the *HAP1* library, and
245 just over 20,000 genes in the *Cortex* library (Supplementary Figure 2). Among the genes for which the score can
246 not be calculated, most are not expressed (predicted total abundance of all isoforms equal to 0), while a smaller
247 fraction either are expressed but lack junctions, or contain junctions but have no or too few uniquely mapping
248 junction-spanning reads to calculate the score.

249 Investigating the overall distribution of valid JCC scores shows that for most genes, the score is low (below
250 0.5), confirming the previous observation that for most of the genes, the junction coverage pattern induced by
251 the estimated transcript abundances agrees well with the observed junction coverages (Figure 2B, left column).
252 Similar distributions are seen for all included methods. Most of the very high scores are obtained for genes
253 with low abundance and few uniquely mapped reads spanning any of the junctions (Figure 2B). The high
254 score for these genes may be driven largely by shot noise, and may improve with even higher sequencing
255 depth. Moreover, lowly expressed genes are typically excluded in practical analyses of RNA-seq data such as
256 differential expression analyses. Thus, to illustrate the behaviour of the JCC score, in the following analyses we
257 focus on genes with at least 25 reads mapping uniquely across any of its junctions.

258 **Examples of genes with high JCC score**

259 In order to exemplify the types of deviating patterns resulting in high JCC scores, we consider some of the
260 genes that are assigned high scores ($JCC \geq 0.6$) with all the transcript abundance methods (except SalmonCDS,
261 since it is based on a different set of reference transcripts and does not represent a typical or recommended way
262 of performing transcript abundance estimation). Furthermore, we limit the investigation to genes with at least

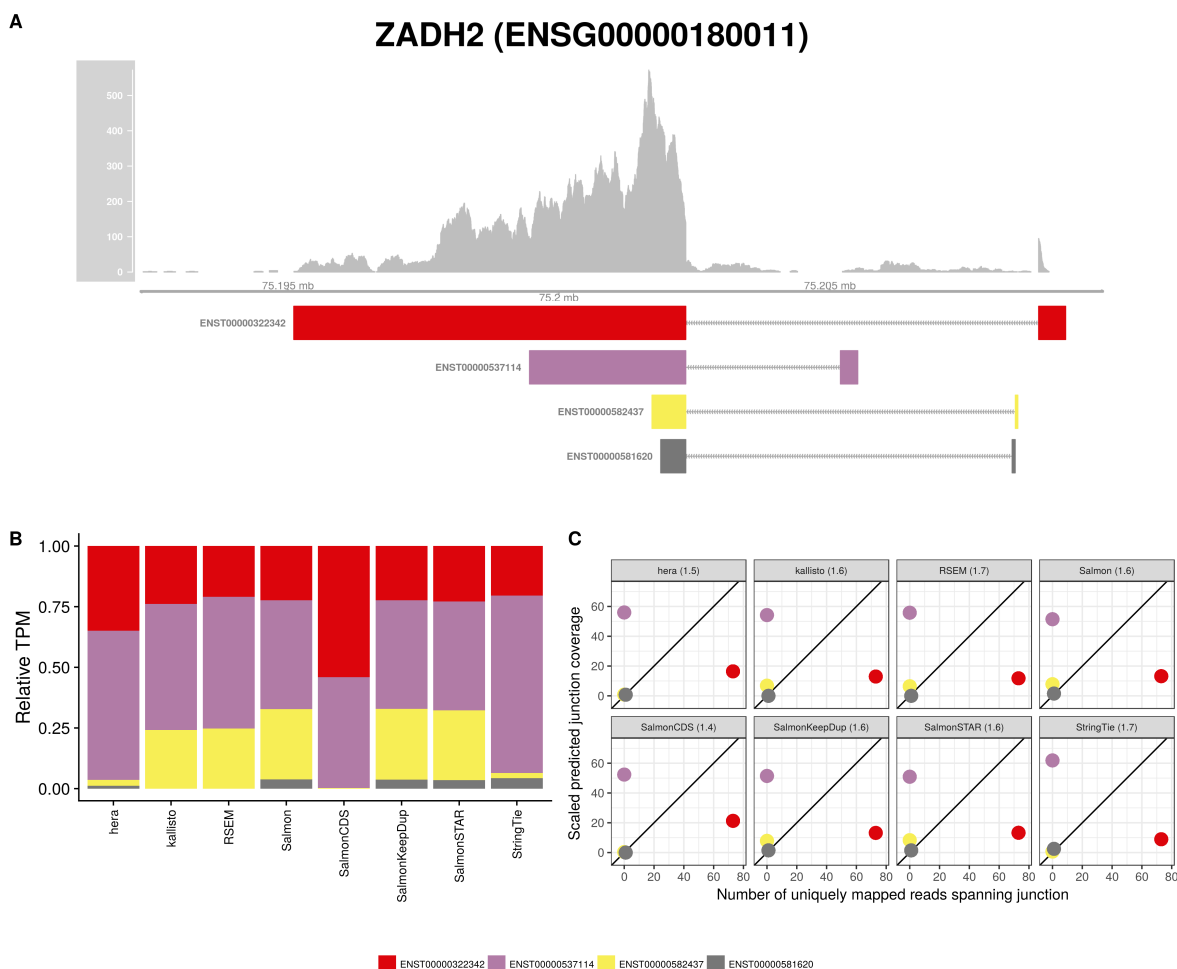


Figure 3: **A.** Observed coverage profile and annotated gene model for the ZADH2 gene in the *HAP1* library. Different annotated transcripts are shown in different color. **B.** Relative TPM estimates for the annotated transcripts from each of the eight transcript abundance estimation methods. **C.** Observed number of uniquely mapping junction-spanning reads (x) and scaled predicted junction coverages (y) based on transcript abundance estimates from each of the eight methods. Each circle corresponds to an annotated junction and is colored according to the set of transcripts that it is annotated to. The JCC scores for this gene based on the respectively abundances are indicated in the panel headers.

263 25 uniquely mapped junction-spanning reads, at least 75% of the junction-spanning reads mapping uniquely
 264 and an intron/exon read count ratio below 0.1. These strict filtering criteria are satisfied by 146 genes in the
 265 *Cortex* library and 56 genes in the *HAP1* library. 17 of the genes passed the filters in both libraries. One of
 266 these genes is ZADH2 (Figure 3, other examples in Supplementary Figures 3-4). ZADH2 has four annotated
 267 transcripts, each consisting of two exons and one junction, and no junction is shared between transcripts. Most
 268 transcript abundance estimation methods distribute the estimated abundance between two or three of these
 269 isoforms. However, only one of the four annotated junctions has any observed spanning reads, which suggests
 270 that only the corresponding transcript (ENST00000322342) is indeed present. This leads to a large discrepancy
 271 between the observed and predicted junction coverages (for all abundance estimation methods), and hence a
 272 large JCC score. For this gene, a possible explanation for the discrepancy is that the coverage of the 5' end of the
 273 transcripts is weak, but for a reason not captured by the alpine bias model, implying that the 3' end, which is

274 longer and shows a higher coverage, will dominate the abundance estimation. Uneven coverage in this region
275 can therefore bias the abundance estimation towards one or the other transcript. As illustrated in Figure 1A, a
276 similar behaviour can be seen also in the GTEx data (accessed via the GTEx Portal).

277 Similar observations can be made for many of the other selected example genes (Supplementary Figures
278 3-4). For many of the high-scoring genes, no distribution of the reads between the annotated transcripts would
279 lead to compatible coverage of both the internal structure (junctions) and the UTRs. For other genes with high
280 scores, we observe a read coverage that is largely incompatible with the annotated exons (e.g., Supplementary
281 Figure 5). In particular, these genes have large numbers of intronic reads, which can not be accounted for by
282 annotated transcripts. This suggests that high scores can often be attributed to incorrectness or incompleteness
283 of the annotation catalog with respect to the observed reads, rather than poor performance of the abundance
284 estimation methods. Regardless of the cause, however, the resulting abundances are unreliable and should be
285 interpreted with caution in downstream analyses.

286 **JCC scores are not strongly associated with inferential variability**

287 Several isoform abundance estimation methods allow assessment of the variability of the resulting expression
288 levels via some form of (re)sampling [9, 10, 15, 16, 36, 37]. In order to compare the uncertainties picked up
289 by the JCC score to those represented in these inferential variances, we perform 100 bootstrap runs using
290 Salmon, and estimate the coefficient of variation of the bootstrapped counts both on the transcript level and
291 after aggregating the transcript counts on the gene level. For the evaluation, we consider only genes with at
292 least 25 uniquely mapping junction-spanning reads, and each individual transcript is assigned the JCC score
293 of the corresponding gene. Overall, the association between the inferential coefficient of variation and the JCC
294 score is weak in both libraries, on both the transcript and gene level (Supplementary Figure 6). Thus, the
295 two scores measure different types of uncertainties; while the bootstrap variability may capture assignment
296 uncertainty caused by shared sequence features among transcripts, it will not in general pick up inconsistencies
297 due to misannotation, which are targeted by the JCC score.

298 **JCC scores are overall similar between methods**

299 Since the JCC score is obtained by combining a set of estimated transcript coverage profiles with transcript
300 abundance estimates, using different transcript abundance methods for the latter leads to different sets of scores.
301 We calculate JCC scores using transcript abundance estimates from eight different methods, and the results
302 shown above illustrate that all of them suffer from problems induced by misannotated or missing transcripts,
303 leading to predicted junction coverages that are incompatible with the observed ones. To further investigate
304 the similarities between the methods, we calculate correlation coefficients between the scores obtained by each
305 method pair, using only genes with at least 25 uniquely mapping junction-spanning reads (Supplementary
306 Figures 7-9). As expected, the correlation is overall very high, and the most deviating scores are obtained
307 with SalmonCDS, which uses a different set of reference sequences than the other methods, and StringTie. On
308 average, both SalmonCDS and StringTie give higher scores than the remaining methods (Supplementary Figure
309 9B).

310 **The choice of reference annotation affects the JCC score distribution**

311 All analyses so far have been performed using the Ensembl GRCh38.90 annotation. To investigate the im-
312 pact of the choice of reference annotation on the JCC scores, we estimate bias models and predict transcript
313 coverage profiles also for all transcripts in the CHES 2.0 catalog [26]. We estimate corresponding transcript

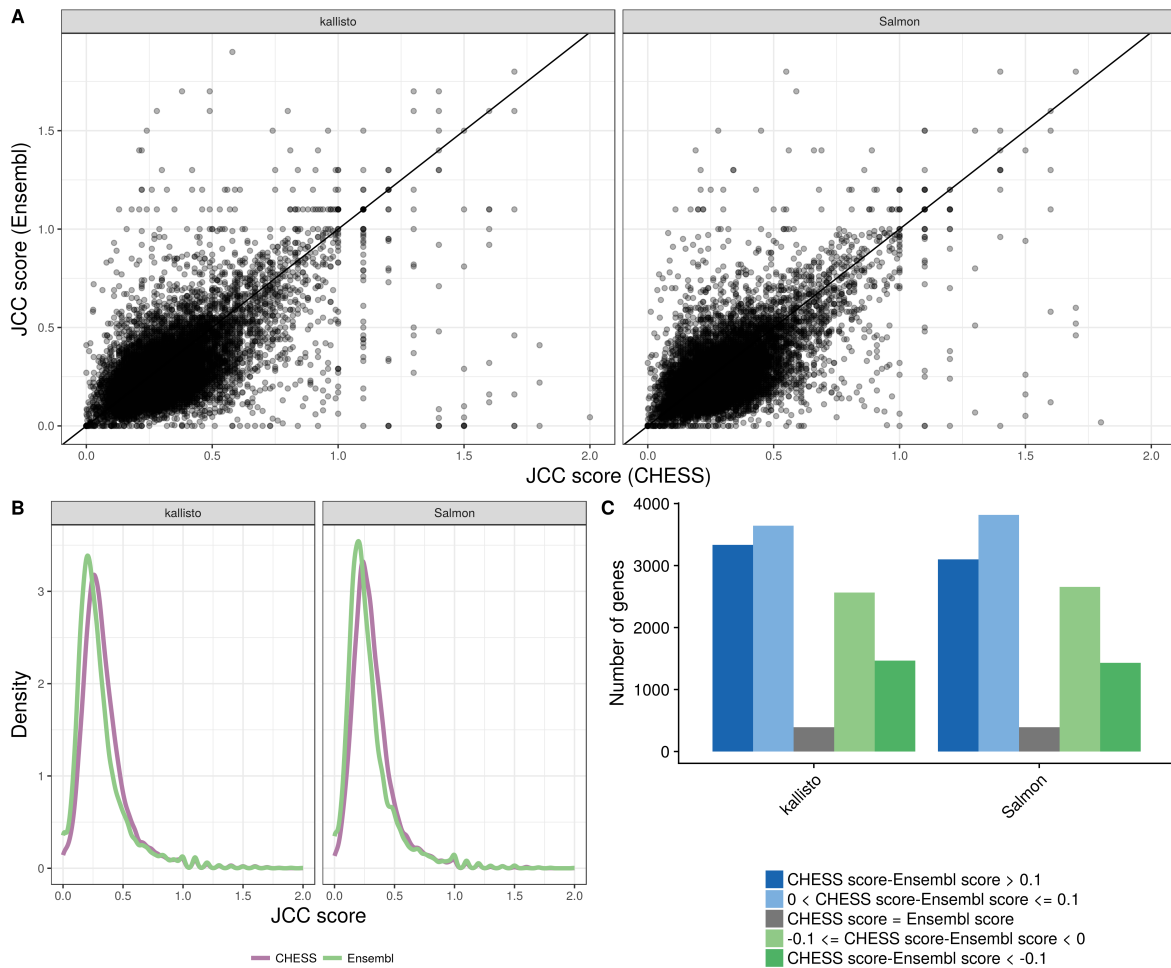


Figure 4: Comparison between scores obtained with the Ensembl GRCh38.90 annotation and the CHES 2.0 annotation, for the *HAP1* sample. **A**. Correlation between scores obtained with the CHES annotation (x) and the Ensembl annotation (y), for all the shared genes (genes with an assigned Ensembl ID in the CHES catalog), with at least 25 uniquely mapping junction-spanning reads and at least 75% of the junction-spanning reads mapping uniquely with both annotations. **B**. Distribution of JCC scores for all genes with at least 25 uniquely mapping junction-spanning reads and at least 75% of the junction-spanning reads mapping uniquely, in the respective annotation catalogs. **C**. The number of genes shared between the two annotation catalogs for which the CHES annotation results in a higher, lower or equal score compared the Ensembl annotation. Blue bars represent genes for which scores based on the CHES annotation are higher (worse) than those based on the Ensembl annotation, and green bars represent the opposite situation.

314 abundances with Salmon and kallisto, and count junction-spanning reads for each annotated junction with
 315 STAR. The CHES catalog is obtained by assembling reads from almost 10,000 GTEx samples, and contains a
 316 larger number of transcripts (annotated to a smaller number of genes) than the Ensembl catalog (Supplemen-
 317 tary Table 1). The CHES genes are all annotated with a unique CHES identifier, but a mapping to Entrez IDs
 318 is provided wherever possible. For comparison with our other results, we convert the Entrez IDs to Ensembl
 319 IDs using the `org.Hs.eg.db` Bioconductor package v3.6.0 (in this way, unique Ensembl IDs are obtained for
 320 22,262/42,881=51.9% of the genes). Considering only genes that are shared between the two annotation cata-
 321 logs, it is clear that there is a substantial difference between the scores assigned to an individual gene using the

322 two annotations (Figure 4A), although the overall distribution of scores is largely similar (Figure 4B). Neither
323 annotation catalog is consistently leading to lower scores than the other (Figure 4C), but there are genes with
324 substantially lower scores with each of the two annotations compared to the other.

325 In addition, we investigate the effect of quantifying transcript abundances using a dataset-specific catalog
326 of transcripts, obtained by running StringTie (without the `-e` argument) on each of the two Illumina libraries.
327 The resulting gtf file contains many new transcripts, and many annotated transcripts from the Ensembl cat-
328 alog are removed (Supplementary Table 1). We apply a subset of the abundance estimation methods to the
329 respective StringTie annotations, and compare JCC scores across all genes present in both the StringTie and
330 Ensembl catalogs. Also in this case, no annotation consistently lead to lower scores than the other, but there
331 is a larger fraction of genes that show lower scores with the sample-specific StringTie-assembled annotation
332 (Supplementary Figure 10).

333 **Misannotated 3'UTRs strongly affect the abundance estimates**

334 To investigate the effect of misannotated or missing 3'UTRs on the transcript abundance estimates, and conse-
335 quently the JCC score, in more detail, we used synthetic data. For each of 4,514 annotated genes, we generated
336 an artificial transcript consisting of the coding sequence of one isoform and the 3'UTR of another isoform from
337 the same gene. The two contributing isoforms were selected in such a way that one was annotated with a short
338 3'UTR, and the other with a long 3'UTR (with a length difference of at least 1kb) starting in the same genomic
339 location. As expected, for genes where the isoform with the long 3'UTR was selected to contribute the 3'UTR to
340 the artificial transcript, a large fraction of the final artificial transcript consists of the 3'UTR, while the fraction
341 is much smaller if the 3'UTR was chosen from the isoform with the short 3'UTR (Supplementary Figure 11).

342 For the modified genes, reads are simulated only from the artificial transcript. We also simulate reads
343 from a random selection of unmodified transcripts. As expected, the JCC scores for the genes with modified
344 transcripts are generally higher than those for the genes without any modified transcripts, where the reads are
345 simulated from the correct annotation catalog. The distribution of scores for the latter set of genes can be seen
346 as a “baseline distribution” of scores that we can expect for reasons unrelated to annotation and sequencing
347 artifacts (e.g., sequence similarity causing problems for abundance estimation methods). Furthermore, the JCC
348 score is generally higher for genes where a larger fraction of the artificial transcript is made up of the 3'UTR
349 (Supplementary Figure 12). Focusing only on the genes with modified transcripts, we calculate the similarity
350 between the artificial transcript and all annotated transcripts from the same gene. The similarity is defined
351 by the Jaccard index of the nucleotide positions covered by the two compared transcripts. We stratify the
352 genes based on whether the most similar transcript to the artificial transcript is the one that contributed the
353 internal structure, the one that contributed the 3'UTR, or another one of the annotated transcripts. For most
354 abundance estimation methods, the annotated transcript that is most similar to the artificial transcript (from
355 which the reads were generated) is also assigned the highest expression estimate (Figure 5). The exceptions
356 are SalmonCDS and StringTie, which both generally assign the highest abundance to the transcript that is most
357 similar to the artificial transcript in terms of the internal structure, rather than based on overall similarity.

358 **Discussion and Conclusions**

359 We have described the junction coverage compatibility (JCC) score and shown how it can be used to identify
360 genes or genomic regions where junction coverage patterns predicted from estimated transcript abundances are
361 incompatible with those observed after alignment of the RNA-seq reads directly to the genome. By using the
362 RNA-seq data to obtain two estimates of the number of reads mapping across each splice junction, we can create

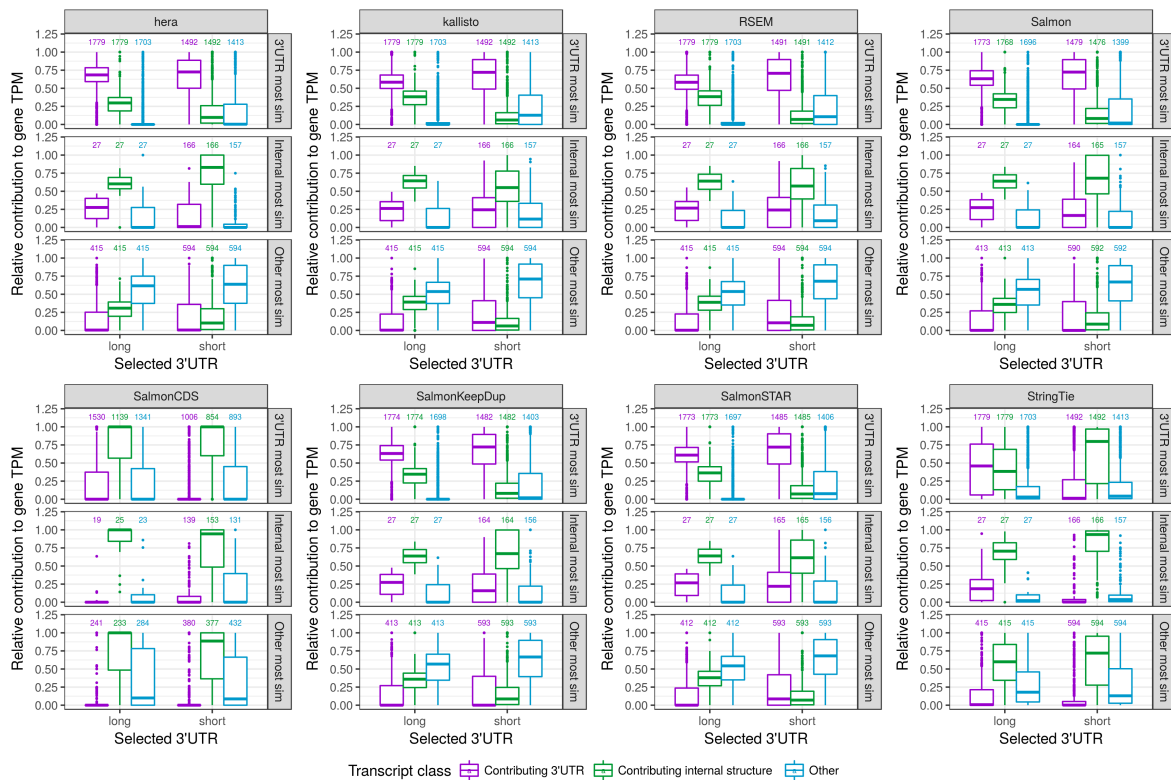


Figure 5: Relative transcript abundances for modified genes, with each of the eight transcript abundance estimation methods. Genes are stratified (vertically) based on whether the transcript that is most similar (by Jaccard index of covered nucleotides) to the artificial transcript is the one contributing the 3'UTR, the one contributing the internal structure, or another isoform of the gene (see Figure 1C). For each gene we calculate the relative abundance of the transcript contributing the 3'UTR, the one contributing the internal structure, and all other isoforms of the gene combined (indicated with color). Finally, genes are stratified (horizontally) based on whether the artificial transcript contains the long or short variant of the 3'UTR. Generally, most methods assign the highest abundance to the transcript that is most similar to the artificial transcript from which the reads were generated, with the exception of SalmonCDS and StringTie, which assign higher abundances to the transcripts that are most similar to the artificial transcript in terms of the internal structure. The numbers above the boxplots indicate the number of genes in each category.

363 an internal validation system, thereby circumventing the need for an external data set or additional replicates
 364 for evaluation of transcript abundance estimation accuracy. A high score, indicating poor compatibility between
 365 the junction coverages estimated from the transcript abundance estimates and the observed junction coverages,
 366 can be caused, e.g., by inaccurate transcript abundance estimates (e.g., for transcripts that share large parts of
 367 their sequence with other transcripts), or by an incomplete or incorrect transcriptome annotation. Regardless
 368 of the underlying cause, such genes should be flagged in downstream analyses and the estimated transcript
 369 abundances interpreted with caution. We note that the results were overall similar for all the eight transcript
 370 abundance estimation tools used in the study, representing alignment-free methods as well as methods relying
 371 on either genome or transcriptome alignments.

372 The chosen reference annotation can have a large effect on the resulting JCC scores, as seen here by compar-
 373 ing the scores obtained using the Ensembl annotation to those based on the CHES 2.0 annotation. In addition,
 374 using StringTie to assemble missing transcripts led to improved scores for a large number of genes, and a worse

375 score for a smaller number of genes. As recommended¹, we used the primary genome assembly from Ensembl
376 for aligning the reads to the genome. However, the transcriptome fasta files from Ensembl, which were used
377 as the basis for abundance estimation by Salmon, SalmonKeepDup, kallisto, RSEM and SalmonSTAR, contain
378 transcripts from alternative contigs that are not included in the primary genome assembly. Many of these tran-
379 scripts are identical or very similar to transcripts annotated to the primary chromosomes. While this represents
380 the typical use of these alignment files for alignment and transcript abundance estimation, it may lead to prob-
381 lems for the correct assignment of the reads to transcripts, and as a consequence, for the calculation of the JCC
382 scores. Keeping only one representative of duplicate transcript sequences (the default behaviour of Salmon)
383 can lead to both better abundance estimates and improved agreement between predicted and observed junction
384 coverages, under the assumption that the correct transcript location is retained. Of course, determining the true
385 location of origin of a given transcript can be highly non-trivial, but would be an interesting direction for future
386 research.

387 One limitation of the presented family of JCC scores is that they can not be calculated for genes that do
388 not have annotated junctions, or that do not have reads spanning junctions. A solution to this could be to
389 compare the predicted and observed coverage profiles of the entire genomic locus rather than just the junctions.
390 However, multimapping reads will still pose a problem for the comparison, and positions with a large fraction
391 of multimapping overlapping reads should be downweighted in the score. In general, the approach we propose
392 is not limited to junction coverages, and could be extended to, e.g., disjoint exon bins. The requirement is that
393 we can observe the coverage pattern of the features of interest from the genome alignment, and predict it from
394 the `alpine` bias models and the estimated transcript abundances. In addition, while we use the weighting
395 function $g(\omega)$ to downweight the influence of junctions with a large fraction of multi-mapping reads, it can be
396 used more generally to assign weights to junctions based on any characteristics affecting our confidence in the
397 observed read coverages.

398 Our evaluations are based on the assumption that we are interested in obtaining and using transcript abun-
399 dance estimates. Other quantification approaches, for example, those focusing on disjoint exon bins [38] or
400 transcript equivalence classes [39] have been suggested, and the resulting counts may in themselves be less
401 sensitive to uncertainties in the reference transcript catalog. However, a post-processing step is required in
402 order to interpret the results in terms of known transcripts, and during this step, misannotated transcripts can
403 still lead to erroneous conclusions.

404 Using simulated data, we observed that compared to the other abundance estimation methods, StringTie
405 appeared to focus more on matching the internal structure than the 3'UTR when assigning abundances to tran-
406 scripts. This implies that in situations where the 3'UTR annotation is unclear, StringTie can help assigning the
407 reads to the transcript that is most similar with respect to the more unambiguous part of the transcript struc-
408 ture. However, it could potentially also make it more difficult to identify differences in transcript composition
409 between tissues, since these have been shown to be predominantly differences in transcription start and end
410 sites [24].

411 Our results show that for the vast majority of the human genes, the junction coverage patterns implied by the
412 estimated transcript abundances in our data sets agree well with the observed ones, indicating that the reference
413 annotation as well as the transcript abundance estimates for these genes are likely to be reliable. However, for
414 each transcript abundance estimation method a small number of genes obtained a high JCC score, suggesting
415 unreliably quantified isoforms. These genes should be treated with care in any downstream analyses, or be
416 investigated further for an improved transcriptome annotation.

¹e.g., <https://github.com/alexandobin/STAR/blob/2.5.3a/doc/STARmanual.pdf>

417 Funding

418 The authors would like to acknowledge support from a Pilot Project grant from the URPP Evolution in Ac-
419 tion of the University of Zurich (to C.S.), the National Science Foundation (BIO-1564917 and CCF-1750472, to
420 R.P.), the National Human Genome Research Institute (R01HG009125, to M.I.L), the National Cancer Institute
421 (P01CA142538, to M.I.L), and the National Institute of Environmental Health Sciences (P30 ES010126, to M.I.L).

422 Acknowledgements

423 The authors would like to thank the members of the Robinson, von Mering and Baudis groups at the University
424 of Zurich for helpful discussions.

425 References

- 426 1. Kanitz, A. *et al.* Comparative assessment of methods for the computational inference of transcript isoform
427 abundance from RNA-seq data. *Genome Biol.* **16**, 150 (2015).
- 428 2. Soneson, C., Love, M. I. & Robinson, M. D. Differential analyses for RNA-seq: transcript-level estimates
429 improve gene-level inferences. *F1000Res.* **4**, 1521 (doi: 10.12688/f1000research.7563.1) (2015).
- 430 3. Paşaniuc, B., Zaitlen, N. & Halperin, E. Accurate estimation of expression levels of homologous genes in
431 RNA-seq experiments. *J. Comput. Biol.* **18**, 459–468 (2011).
- 432 4. Robert, C. & Watson, M. Errors in RNA-Seq quantification affect genes of relevance to human disease.
433 *Genome Biol.* **16**, 177 (2015).
- 434 5. McDermaid, A. *et al.* GeneQC: A quality control tool for gene expression estimation based on RNA-
435 sequencing reads mapping. *bioRxiv* doi:10.1101/266445 (2018).
- 436 6. Wang, X., Wu, Z. & Zhang, X. Isoform abundance inference provides a more accurate estimation of gene
437 expression levels in RNA-seq. *J. Bioinform. Comput. Biol.* **8 Suppl 1**, 177–192 (2010).
- 438 7. Trapnell, C. *et al.* Differential analysis of gene regulation at transcript resolution with RNA-seq. *Nat. Biotech-*
439 *nol.* **31**, 46–53 (2013).
- 440 8. Trapnell, C. *et al.* Transcript assembly and quantification by RNA-Seq reveals unannotated transcripts and
441 isoform switching during cell differentiation. *Nat. Biotechnol.* **28**, 511–515 (2010).
- 442 9. Li, B. & Dewey, C. N. RSEM: accurate transcript quantification from RNA-Seq data with or without a
443 reference genome. *BMC Bioinformatics* **12**, 323 (2011).
- 444 10. Glaus, P., Honkela, A. & Rattray, M. Identifying differentially expressed transcripts from RNA-seq data
445 with biological variation. *Bioinformatics* **28**, 1721–1728 (2012).
- 446 11. Roberts, A. & Pachter, L. Streaming fragment assignment for real-time analysis of sequencing experiments.
447 *Nat. Methods* **10**, 71–73 (2013).
- 448 12. Patro, R., Mount, S. M. & Kingsford, C. Sailfish enables alignment-free isoform quantification from RNA-
449 seq reads using lightweight algorithms. *Nat. Biotechnol.* **32**, 462–464 (2014).
- 450 13. Lee, S., Seo, C. H., Alver, B. H., Lee, S. & Park, P. J. EMSAR: estimation of transcript abundance from
451 RNA-seq data by mappability-based segmentation and reclustering. *BMC Bioinformatics* **16**, 278 (2015).
- 452 14. Pertea, M. *et al.* StringTie enables improved reconstruction of a transcriptome from RNA-seq reads. *Nat.*
453 *Biotechnol.* **33** (2015).

- 454 15. Bray, N. L., Pimentel, H., Melsted, P. & Pachter, L. Near-optimal probabilistic RNA-seq quantification. *Nat.*
455 *Biotechnol.* **34**, 525 (2016).
- 456 16. Patro, R., Duggal, G., Love, M. I., Irizarry, R. A. & Kingsford, C. Salmon provides fast and bias-aware
457 quantification of transcript expression. *Nat. Methods* **14**, 417 (2017).
- 458 17. Liu, R. & Dickerson, J. Strawberry: Fast and accurate genome-guided transcript reconstruction and quan-
459 tification from RNA-Seq. *PLoS Comput. Biol.* **13**, e1005851 (2017).
- 460 18. Leshkowitz, D. *et al.* Using Synthetic Mouse Spike-In Transcripts to Evaluate RNA-Seq Analysis Tools.
461 *PLoS One*, 1–20 (2016).
- 462 19. Teng, M. *et al.* A benchmark for RNA-seq quantification pipelines. *Genome Biol.* **17**, 74 (2016).
- 463 20. Dapas, M., Kandpal, M., Bi, Y. & Davuluri, R. V. Comparative evaluation of isoform-level gene expression
464 estimation algorithms for RNA-seq and exon-array platforms. *Brief. Bioinform.* bbw016 (2016).
- 465 21. Zhang, R. *et al.* AtRTD - a comprehensive reference transcript dataset resource for accurate quantification
466 of transcript-specific expression in *Arabidopsis thaliana*. *New Phytol.* **208**, 96–101 (2015).
- 467 22. Pal, S. *et al.* Alternative transcription exceeds alternative splicing in generating the transcriptome diversity
468 of cerebellar development. *Genome Res.* **21**, 1260–1272 (2011).
- 469 23. Shabalina, S. A., Ogurtsov, A. Y., Spiridonov, N. A. & Koonin, E. V. Evolution at protein ends: major
470 contribution of alternative transcription initiation and termination to the transcriptome and proteome
471 diversity in mammals. *Nucleic Acids Res.* **42**, 7132–7144 (2014).
- 472 24. Reyes, A. & Huber, W. Alternative start and termination sites of transcription drive most transcript isoform
473 differences across human tissues. *Nucleic Acids Res.* **46**, 582–592 (2018).
- 474 25. Zerbino, D. R. *et al.* Ensembl 2018. *Nucleic Acids Res.* **46**, D754–D761 (2018).
- 475 26. Pertea, M. *et al.* Thousands of large-scale RNA sequencing experiments yield a comprehensive new human
476 gene list and reveal extensive transcriptional noise. *bioRxiv doi:10.1101/332825* (2018).
- 477 27. GTEx Consortium. The Genotype-Tissue Expression (GTEx) project. *Nat. Genet.* **45**, 580–585 (2013).
- 478 28. Carithers, L. J. *et al.* A Novel Approach to High-Quality Postmortem Tissue Procurement: The GTEx
479 Project. *Biopreserv. Biobank.* **13**, 311–319 (2015).
- 480 29. Liao, Y., Smyth, G. K. & Shi, W. featureCounts: an efficient general purpose program for assigning sequence
481 reads to genomic features. *Bioinformatics* **30**, 923–930 (2014).
- 482 30. Liao, Y., Smyth, G. K. & Shi, W. The Subread aligner: fast, accurate and scalable read mapping by seed-
483 and-vote. *Nucleic Acids Res.* **41**, e108 (2013).
- 484 31. Frazee, A. C., Jaffe, A. E., Langmead, B. & Leek, J. T. Polyester: simulating RNA-seq datasets with differ-
485 ential transcript expression. *Bioinformatics* **31**, 2778–2784 (2015).
- 486 32. Langmead, B., Trapnell, C., Pop, M. & Salzberg, S. L. Ultrafast and memory-efficient alignment of short
487 DNA sequences to the human genome. *Genome Biol.* **10**, R25 (2009).
- 488 33. Kim, D., Langmead, B. & Salzberg, S. L. HISAT: a fast spliced aligner with low memory requirements. *Nat.*
489 *Methods* **12**, 357 (2015).
- 490 34. Dobin, A. *et al.* STAR: ultrafast universal RNA-seq aligner. *Bioinformatics* **29**, 15–21 (2013).
- 491 35. Love, M. I., Hogenesch, J. B. & Irizarry, R. A. Modeling of RNA-seq fragment sequence bias reduces
492 systematic errors in transcript abundance estimation. *Nat. Biotechnol.* **34**, 1287–1291 (2016).

- 493 36. Turro, E., Astle, W. J. & Tavaré, S. Flexible analysis of RNA-seq data using mixed effects models. *Bioinform-*
494 *atics* **30**, 180–188 (2014).
- 495 37. Mandric, I. *et al.* Fast Bootstrapping-Based Estimation of Confidence Intervals of Expression Levels and
496 Differential Expression from RNA-Seq Data. *Bioinformatics* (2017).
- 497 38. Anders, S., Reyes, A. & Huber, W. Detecting differential usage of exons from RNA-seq data. *Genome Res.*
498 **22**, 2008–2017 (2012).
- 499 39. Ntranos, V., Kamath, G. M., Zhang, J. M., Pachter, L. & Tse, D. N. Fast and accurate single-cell RNA-seq
500 analysis by clustering of transcript-compatibility counts. *Genome Biol.* **17**, 112 (2016).